MATHEMATICAL MODELING AND COMPUTING, Vol. 11, No. 1, pp. 277–289 (2024)

Scattered data interpolation on the 2-dimensional surface through Shepard-like technique

Zerroudi B.[1], Tayeq H.[2,3], El Harrak A.[3]

[1] *Laboratory of Engineering Sciences, Faculty of Science, Ibn Zohr University, Agadir, Morocco*
[2] *SMAD, FPL, Abdelmalek Essaadi University, Tetouan, Morocco*
[3] *MMA, FPL, Abdelmalek Essaadi University, Tetouan, Morocco*

(Received 27 June 2023; Accepted 29 February 2024)

In the current paper, the problem of interpolation of scattered data on two-dimensional surfaces is considered by proposing an extension to the Shepard method and its modified version to surfaces. Each proposed operator is a linear combination of basis functions whose coefficients are the values of the function or its Taylor of first-order expansions at the interpolation points using both functional and derivative data. Numerical tests are given to show the interpolation performance, where several numerical results show a good approximation accuracy of the proposed operator.

Keywords: *scattered data interpolation; interpolation algorithms; Shepard methods; manifolds approximation; surface triangle.*

2010 MSC: 65D05, 65D15 **DOI:** 10.23939/mmc2024.01.277

1. Introduction

Since ancient times, there has been a great deal of research on the topic of scattered data approximation using finite measurements of the function [1]. This problem arises in a variety of fields where the data typically represent some physical phenomena, such as temperature, rainfall, or elevation, observed at various points on a surface. It is often impractical to obtain data at all of the points at which values are desired, thus necessitating an approximation technique such as interpolation.

When the data are confined to a plane region, the problem becomes that of bivariate interpolation for arbitrarily distributed points in the plane. Here, this case was treated in different ways by several authors. D. Shepard introduced a solution to this problem in the late 60s, in the famous paper [2]. After that, many studies have investigated how to enhance the reproduction quality of the Shepard operator utilizing different forms of weight functions to overcome the disadvantages of the original Shepard method [3, 4]. On the other hand, to maintain the advantages of the original Shepard method, many studies are carried out to increase the reproduction quality of the Shepard operator in the presence of different types of functional and derivative data [5–7]. As solutions to these problems, or even more complex ones, many methods are proposed, such as splines, supersplines, radial basis functions, and Shepard-like methods. The Shepard interpolation method has proven its efficiency and reliability in several works and has applications for the prediction of dynamical and equilibrium properties of the Born–Oppenheimer potential energy surface of a molecular system [8] and in the use of an inverse problem of residual fields [9].

On the other hand, when the data are distributed on a surface (sphere, cylinder, cone, or any general surface), many methods are proposed in the literature. With regard to the spherical interpolation problem, many methods have been proposed to solve the spherical interpolation problem for scattered data. In fact, it would take extensive effort to compile a list of the various methods which have been proposed for this problem. Some of these methods include spherical harmonics, spherical analogues of thin plate splines, tensor splines, and radial basis functions [10–18] among others. Many studies have also considered the approximation problem in the general case of Riemannian manifolds (see [19–22]).

The purpose of this paper is to generalize the results for Shepard-like interpolation. Here, we consider an extended version of the Shepard methods in 2-dimensional surfaces in $\mathbb{R}^3$. In fact, we preserve all the advantages of the Shepherd method, in which the interpolant is directly expressed as a linear combination of basis functions, which depend on the geodesic distance. Also, the basis functions have many important properties, such as its derivative equal to zero at the interpolation points. We refer to the fact that we rely on two types of basis function, the first one is the point basis function, the coefficients of the linear combination in this case are values of the unknown function. As for the second type of basis functions which are the triangular basis functions, the coefficients of the linear combination, in this case, are local interpolants over triangles. The results proven in this paper can be used in several fields, especially when modeling concrete surfaces such as maritime traffic, GPS satellites, and any problem that requires good precision interpolation of $3D$ positions [23].

This paper is organized as follows. In Section 2, we present the interpolation problem on general surfaces in $\mathbb{R}^3$ and introduce the interpolant, which is based on a suitable class of cardinal basis functions that depend only on geodesic distances. In Section 3, we give the basis function based on the triangulation, and we present two local interpolants over each triangle. By using the linear combination of triangular basis functions and local interpolants, we present two operators. In Section 4, we discuss numerical tests on some surfaces which are the most interesting and handy cases, such as a sphere, cone, and cylinder, but the adopted point of view is more general. The consideration of these surfaces in the numerical test relies on the availability of the explicit expression of the geodesic distance.

2. Shepard basis functions on general surface

In this paper, we note by $\mathcal{M}$ a surface in $\mathbb{R}^3$ defined by $\mathcal{M} = \{(x, y, z) \in \mathbb{R}^3; z = F(x, y)\}$, $\Omega = \{\boldsymbol{u} = (u_1, u_2, u_3) \in \mathbb{R}^3\} \subset \mathcal{M}$ is an open geodesically convex, and $\varphi\colon \Omega \to \mathbb{R}^2$ is a function that maps Ω homeomorphically to the open set $\Lambda = \{\boldsymbol{x} = (x_1, x_2) \in \mathbb{R}^2\}$. Given a set of distinct points $X = \{\boldsymbol{u}_1, \ldots, \boldsymbol{u}_n\}$, arbitrarily distributed on Ω, with associated data f_i sampled from some unknown function $f\colon \Omega \to \mathbb{R}$, such that $f_i = f(\boldsymbol{u}_i)$, $i = 1, \ldots, n$.

For any $u_i \in \Omega$, $i = 1, \ldots, n$, there exists only one $x_i \in \Lambda$ such that $\varphi(\boldsymbol{u}_i) = \boldsymbol{x}_i$, and we consider the following notations:

$$\nabla_{\boldsymbol{x}} f := \left(\frac{\partial f}{\partial x_1}, \frac{\partial f}{\partial x_2}\right) \quad \text{and} \quad D_{\boldsymbol{u}-\boldsymbol{u}_i} f(\boldsymbol{u}_i) := (\boldsymbol{x} - \boldsymbol{x}_i) \cdot \nabla_{\boldsymbol{x}} f,$$

where "$\cdot$" denotes the scalar product in $\mathbb{R}^2$. To construct the basis function, we need to define the geodesic distance between two points on $\mathcal{M}$ [24]. For this reason, let be $\boldsymbol{A}$ and $\boldsymbol{B}$ two points on $\mathcal{M}$ and $\gamma\colon [0, 1] \to \mathcal{M}$ a C^1 curve between $\boldsymbol{A}$ and $\boldsymbol{B}$, that is $\gamma(0) = \boldsymbol{A}$ and $\gamma(1) = \boldsymbol{B}$, the γ length given as

$$L[\boldsymbol{A}, \boldsymbol{B}, \gamma] = \int_0^1 \|\gamma'(t)\|_{\mathbb{R}^3} dt.$$

Supposing $\varphi(\Omega)$ be compact in $\mathbb{R}^2$, the geodesic distance between $\boldsymbol{A} \in \Omega$ and $\boldsymbol{B} \in \Omega$ denoted by $d_g(\boldsymbol{A}, \boldsymbol{B})$ is the length of the shortest of all curves connecting $\boldsymbol{A}$ and $\boldsymbol{B}$. By $C(\Omega)$, we denote the class of all real-valued continuous functions on Ω. We note Δ the projection of the region $D \subset \mathcal{M}$ on the plane xoy, the surface area of D is [25]

$$\text{area}(D) := \int_\Delta \sqrt{1 + F_x'^2 + F_y'^2}\, dx\, dy,$$

where

$$F_x' = \frac{\partial F}{\partial x} \quad \text{and} \quad F_y' = \frac{\partial F}{\partial y}.$$

In order to build a function $S_\mu[f]$ defined on Ω which interpolates the data, namely,

$$S_\mu[f](\boldsymbol{u}_i) = f_i, \quad i = 1, \ldots, n,$$

we can consider, in line with classical Shepard operator in the Euclidean space [5], an interpolant defend on Ω by the form

$$S_\mu[f](\boldsymbol{u}) = \sum_{i=1}^{n} A_{\mu,i}(\boldsymbol{u}) f_i, \quad \boldsymbol{u} \in \Omega. \tag{1}$$

This interpolant uses point-based basis functions

$$A_{\mu,i}(u) = \frac{(d_g(\boldsymbol{u}, \boldsymbol{u}_i))^{-\mu}}{\sum_{k=1}^{n} (d_g(\boldsymbol{u}, \boldsymbol{u}_k))^{-\mu}}, \quad i = 1, \ldots, n, \tag{2}$$

where d_g denotes the geodesic metric on $\mathcal{M}$ and μ is a real positive parameter control.

The functions $A_{\mu,i}(\boldsymbol{u})$ are cardinal basis functions; they satisfy for all $\boldsymbol{u} \in \mathcal{M}$ and $i, j = 1, \ldots, n$, the conditions

$$A_{\mu,i}(\boldsymbol{u}) \geqslant 0, \quad \sum_{i=1}^{n} A_{\mu,i}(\boldsymbol{u}) = 1, \quad A_{\mu,i}(\boldsymbol{u}_j) = \delta_{ij},$$

where δ_{ij} is the Kronecker delta.

By construction of the basis functions $A_{\mu,i}(\boldsymbol{u})$, we can easily verify the previous properties. Also, the interpolation properties are satisfied by the interpolant $S_\mu[f]$; (i.e.) for all $i = 1, \ldots, n$, we have

$$S_\mu[f](\boldsymbol{u}_i) = f(\boldsymbol{u}_i).$$

To give more significant error estimates, let us consider $B_r(\boldsymbol{w}) := \{\boldsymbol{u} \in \mathcal{M}; d_g(\boldsymbol{w}, \boldsymbol{u}) \leqslant r\}$ for any $\boldsymbol{w} \in \mathcal{M}$. Since for any $\boldsymbol{u} \in \Omega$ there exists $r_{\boldsymbol{u}} > 0$ such that $B_{r_{\boldsymbol{u}}}(\boldsymbol{u})$ contains at least one element of X, let be $h = \inf\{r_{\boldsymbol{u}}; \boldsymbol{u} \in \Omega\}$. Under these assumptions, for any $\boldsymbol{u} \in \Omega$, $B_h(\boldsymbol{u})$ contains at least one element of X. Let us consider $M = \sup_{\boldsymbol{w} \in \mathcal{M}} \{B_h(\boldsymbol{w}) \cap X\}$. By construction of h, we have $M > 0$.

Proposition 1. Suppose that f is continuous in Ω. Then for any $\mu > 4$, we have

$$|S_\mu[f](\boldsymbol{u}) - f(\boldsymbol{u})| < \omega\, C\, h,$$

where ω is the f modulus continuity and $C = M + C'$ ($C' = \lim \sum_{k=2}^{N} \frac{(2k-1)^2}{(2k-3)^{\mu-1}}$).

Proof. For fixed $\boldsymbol{u} \in \Omega$, $\boldsymbol{u} \neq \boldsymbol{u_i}$ $(i = 1, \ldots, n)$. Since Ω is compact, there exists a smaller non-zero integer N such that $\Omega \subset B_{(2N-1)h}(\boldsymbol{u})$. Now we will group the elements of X in such a way:

- $G_1(\boldsymbol{u}) = \{\boldsymbol{u}_i \in X; d_g(\boldsymbol{u}, \boldsymbol{u}_i) \leqslant h\}$,
- $G_k(\boldsymbol{u}) = \{\boldsymbol{u}_i \in X; (2k-3)h < d_g(\boldsymbol{u}, \boldsymbol{u}_i) \leqslant (2k-1)h\}$, for $k = 2, \ldots, N$.

Each subset $G_k(\boldsymbol{u})$ contains at most $\left[\frac{\mathbf{A}(G_k(\boldsymbol{u}))}{\mathbf{A}(G_1(\boldsymbol{u}))}\right]$ elements of X, where [.] and $\mathbf{A}\big(G_k(\boldsymbol{u})\big)$ denote, respectively, the floor function and area. Therefore, $G_k(\boldsymbol{u})$ contains at most $(2k-1)^2 M$ elements of X.

Now, according the continuities of f, for any $\boldsymbol{u}_i \in X$, we have

$$|f(\boldsymbol{u}) - f(\boldsymbol{u_i})| \leqslant \omega\, d_g(\boldsymbol{u}, \boldsymbol{u}_i), \tag{3}$$

$$\begin{aligned} |S_\mu[f](\boldsymbol{u}) - f(\boldsymbol{u})| &= \left| \sum_{i=1}^{n} A_{\mu,i}(\boldsymbol{u}) f_i - f(\boldsymbol{u}) \right| = \left| \sum_{i=1}^{n} A_{\mu,i}(\boldsymbol{u})(f_i - f(\boldsymbol{u})) \right| \\ &\leqslant \sum_{i=1}^{n} A_{\mu,i}(\boldsymbol{u}) |f(\boldsymbol{u}_i) - f(\boldsymbol{u})| \\ &\leqslant \sum_{\boldsymbol{u}_i \in G_1} A_{\mu,i}(\boldsymbol{u}) |f(\boldsymbol{u}_i) - f(\boldsymbol{u})| + \sum_{k=2}^{N} \sum_{\boldsymbol{u}_i \in G_k} A_{\mu,i}(\boldsymbol{u}) |f(\boldsymbol{u}_i) - f(\boldsymbol{u})|. \end{aligned} \tag{4}$$

According the basis functions properties, the fact that $d_g(\boldsymbol{u}, \boldsymbol{u}_i) \leqslant h$ for any $\boldsymbol{u}_i \in G_1(\boldsymbol{u})$, and the inequality (3), the first term is bounded as

$$\sum_{\boldsymbol{u}_i \in G_1} A_{\mu,i}(\boldsymbol{u}) |f(\boldsymbol{u}_i) - f(\boldsymbol{u})| \leqslant M \omega h. \tag{5}$$

Concerning the second term, we have

$$\sum_{k=2}^{N}\sum_{\boldsymbol{u}_i\in G_k} A_{\mu,i}(\boldsymbol{u})|f(\boldsymbol{u}_i)-f(\boldsymbol{u})| \leqslant \omega \sum_{k=2}^{N}\sum_{\boldsymbol{u}_i\in G_k} A_{\mu,i}(\boldsymbol{u})\, d_g(\boldsymbol{u},\boldsymbol{u}_i)$$
$$\leqslant \omega \frac{\displaystyle\sum_{k=2}^{N}\sum_{\boldsymbol{u}_i\in G_k}(d_g(\boldsymbol{u},\boldsymbol{u}_i))^{-\mu+1}}{\displaystyle\sum_{k=1}^{n}(d_g(\boldsymbol{u},\boldsymbol{u}_k))^{-\mu}} \leqslant \omega \frac{\displaystyle\sum_{k=2}^{N}\sum_{\boldsymbol{u}_i\in G_k}(d_g(\boldsymbol{u},\boldsymbol{u}_i))^{-\mu+1}}{\displaystyle\sum_{\boldsymbol{u}_i\in G_1}(d_g(\boldsymbol{u},\boldsymbol{u}_i))^{-\mu}},$$

we know that for any $\boldsymbol{u}_k \in G_1$, we have $d_g(\boldsymbol{u},\boldsymbol{u}_k) \leqslant h$, which give

$$\frac{1}{\displaystyle\sum_{\boldsymbol{u}_i\in G_1}(d_g(\boldsymbol{u},\boldsymbol{u}_i))^{-\mu}} \leqslant \frac{h^\mu}{M},$$

on the other hand, for any $\boldsymbol{u}_i \in G_k$, $k=2,\ldots,N$, we have $(2k-3)h < d_g(\boldsymbol{u},\boldsymbol{u}_i) \leqslant (2k-1)h$. Under the condition $\mu > 1$, we obtain

$$((2k-1)h)^{-\mu+1} \leqslant (d_g(\boldsymbol{u},\boldsymbol{u}_i))^{-\mu+1} < ((2k-3)h)^{-\mu+1},$$

then, by applying the sum, we find

$$(2k-1)^2 M((2k-1)h)^{-\mu+1} \leqslant \sum_{\boldsymbol{u}_i\in G_k}(d_g(\boldsymbol{u},\boldsymbol{u}_i))^{-\mu+1} < (2k-1)^2 M((2k-3)h)^{-\mu+1},$$

as a result

$$M\sum_{k=2}^{N}(2k-1)^2((2k-1)h)^{-\mu+1} \leqslant \sum_{k=2}^{N}\sum_{\boldsymbol{u}_i\in G_k}(d_g(\boldsymbol{u},\boldsymbol{u}_i))^{-\mu+1} < M\sum_{k=2}^{N}(2k-1)^2((2k-3)h)^{-\mu+1}.$$

Thus, we find the bond

$$\sum_{k=2}^{N}\sum_{\boldsymbol{u}_i\in G_k} A_{\mu,i}(\boldsymbol{u})|f(\boldsymbol{u}_i)-f(\boldsymbol{u})| \leqslant \omega\, h \sum_{k=2}^{N}(2k-1)^2(2k-3)^{-\mu+1}. \tag{6}$$

By substituting (5) and (6) in (4), we obtain

$$|S_\mu[f](\boldsymbol{u}) - f(\boldsymbol{u})| \leqslant \omega\, h\,(M + \sum_{k=2}^{N}(2k-1)^2(2k-3)^{-\mu+1}).$$

If either $\mu > 4$, the sum $S_N = \sum_{k=2}^{N}(2k-1)^2(2k-3)^{-\mu+1}$ converges (bounded by $C' \in \mathbb{R}^+$). Moreover, we have $\left|S_\mu[f](\boldsymbol{u}) - f(\boldsymbol{u})\right| \leqslant \omega\, h\,(M + C')$. ∎

Remark 1. If all the points $\boldsymbol{u_i}$ are in G_1, we will have $|S_\mu[f](\boldsymbol{u}) - f(\boldsymbol{u})| \leqslant M\,\omega\, h$.

3. Surface–triangle–based basis functions

To extend the point-based basis functions in (2) to Surface-triangle-based basis functions, let us consider a surface triangulation $T = \{t_1,\ldots,t_m\}$ of the nodes X. That is, each $t_j = [\boldsymbol{u}_{j_1},\boldsymbol{u}_{j_2},\boldsymbol{u}_{j_3}]$ is a surface triangle with vertices in X and each node $\boldsymbol{u}_i$ is the vertex of at least one surface triangle, hence

$$\cup_j\{j_1,j_2,j_3\} = \{1,2,\ldots,n\}.$$

We note that the set of surface triangulations T can be the *Delaunay triangulation* of X, or it can be a general surface triangulation with overlapping or disjoint surface triangles (Figure 1).

The basis functions corresponding to the surface triangulation T are then defined by

$$\Phi_{\mu,j}(\boldsymbol{u}) = \frac{\displaystyle\prod_{\ell=1}^{3}\frac{1}{(d_g(\boldsymbol{u},\boldsymbol{u}_{j_\ell}))^\mu}}{\displaystyle\sum_{k=1}^{m}\prod_{\ell=1}^{3}\frac{1}{(d_g(\boldsymbol{u},\boldsymbol{u}_{k_\ell}))^\mu}} = \frac{\displaystyle\prod_{k\neq j}\prod_{\ell=1}^{3}(d_g(\boldsymbol{u},\boldsymbol{u}_{k_\ell}))^\mu}{\displaystyle\sum_{k=1}^{m}\prod_{i\neq k}\prod_{\ell=1}^{3}(d_g(\boldsymbol{u},\boldsymbol{u}_{i_\ell}))^\mu}, \quad j=1,\ldots,m. \tag{7}$$

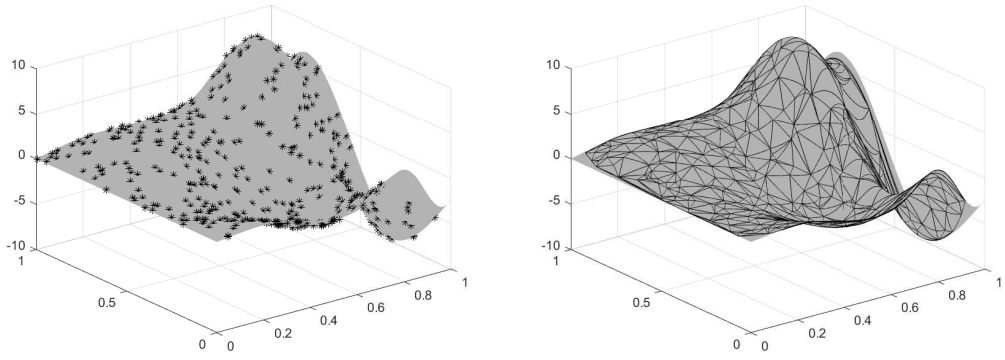

a ***b***

Fig. 1. Set of points on a surface: 400 points (***a***), Delaunay triangulation (786 surface triangles) (***b***).

Note that

$$\Phi_{\mu,j}(\boldsymbol{u}_i) = \delta_{ij}, \qquad \Phi_{\mu,j}(\boldsymbol{u}) \geqslant 0, \qquad \sum_{j=1}^{n} \Phi_{\mu,j}(\boldsymbol{u}) = 1.$$

For any $t_j \in T$, we consider the local basis functions corresponding to t_j given as

$$w_{j,j_1} = \frac{S(\boldsymbol{u}, \boldsymbol{u}_{j_2}, \boldsymbol{u}_{j_3})}{S(\boldsymbol{u}_{j_1}, \boldsymbol{u}_{j_2}, \boldsymbol{u}_{j_3})}, \qquad w_{j,j_2} = \frac{S(\boldsymbol{u}_{j_1}, \boldsymbol{u}, \boldsymbol{u}_{j_3})}{S(\boldsymbol{u}_{j_1}, \boldsymbol{u}_{j_2}, \boldsymbol{u}_{j_3})}, \qquad w_{j,j_3} = \frac{S(\boldsymbol{u}_{j_1}, \boldsymbol{u}_{j_2}, \boldsymbol{u})}{S(\boldsymbol{u}_{j_1}, \boldsymbol{u}_{j_2}, \boldsymbol{u}_{j_3})},$$

where $S(\boldsymbol{u}, \boldsymbol{v}, \boldsymbol{w})$ denotes the signed area of the surface triangle $[\boldsymbol{u}, \boldsymbol{v}, \boldsymbol{w}]$.

We can verify very easy that the basis functions $w_{j,j_\ell}(\boldsymbol{u})$, $\ell = 1, 2, 3$, satisfy the following conditions

$$w_{j,j_\ell}(\boldsymbol{u}_{\boldsymbol{j},\boldsymbol{j_k}}) = \delta_{k\ell}, \quad k, \ell = 1, 2, 3; \tag{8}$$

$$\sum_{\ell=1}^{3} w_{j,j_\ell}(\boldsymbol{u}) = 1 \quad \forall \boldsymbol{u} \in \mathcal{M}, \tag{9}$$

for all $j \in \{1, \ldots, m\}$.

Now, let us define over t_j the following operator

$$H_j[f](\boldsymbol{u}) = \sum_{\ell=1}^{3} w_{j,j_\ell}(\boldsymbol{u}) f_{j_\ell}, \tag{10}$$

locally interpolate the given data at the vertices of each of the triangles.

Proposition 2. For any $f \in C(\Omega)$ and for any $\boldsymbol{u} \in t_j$, $j = 1, \ldots, m$, we have the following bound for the remainder term

$$|f(\boldsymbol{u}) - H_j[f](\boldsymbol{u})| \leqslant \omega\, d_g(\boldsymbol{u}, \boldsymbol{u}_{j_m}),$$

with $d_g(\boldsymbol{u}, \boldsymbol{u}_{j_m}) = \max\{d_g(\boldsymbol{u}, \boldsymbol{u}_{j_\ell}); \ell = 1, 2, 3\}$.

Proof. For any $j = 1, \ldots, m$ and any $\boldsymbol{u} \in t_j$, by using (10), we have

$$\begin{aligned} f(\boldsymbol{u}) - H_j[f](\boldsymbol{u}) &= \sum_{\ell=1}^{3} w_{j,j_\ell}(\boldsymbol{u}) f(\boldsymbol{u}) - \sum_{\ell=1}^{3} w_{j,j_\ell}(\boldsymbol{u}) f_{j_\ell} \\ &= \sum_{\ell=1}^{3} w_{j,j_\ell}(\boldsymbol{u}) \left(f(\boldsymbol{u}) - f_{j_\ell}\right), \end{aligned}$$

by the triangle inequality and the fact that $0 \leqslant w_{j,j_\ell}(\boldsymbol{u})$, $\ell = 1, 2, 3$, then

$$|f(\boldsymbol{u}) - H_j[f](\boldsymbol{u})| \leqslant \sum_{\ell=1}^{3} w_{j,j_\ell}(\boldsymbol{u}) |f(\boldsymbol{u}) - f_{j_\ell}|. \tag{11}$$

According to the continuity of f, for any $\ell = 1, 2, 3$, we gain

$$|f(\boldsymbol{u}) - f_{j_\ell}| \leqslant \omega \|\boldsymbol{u} - \boldsymbol{u}_{j_\ell}\|_{\mathbb{R}^3} \leqslant \omega\, d_g(\boldsymbol{u}, \boldsymbol{u}_{j_\ell}), \tag{12}$$

by substituting (12) in (11), we find

$$\left|f(\boldsymbol{u}) - H_j[f](\boldsymbol{u})\right| \leqslant \omega \sum_{\ell=1}^{3} w_{j,j_\ell}(\boldsymbol{u})\, d_g(\boldsymbol{u}, \boldsymbol{u}_{j_\ell}),$$

then, by using (9), we obtain the Proposition 2. ∎

In the presence of additional the first-order derivatives data, we can enhance the approximation order of $H_j[f]$. If in (10) we replace f_{j_ℓ} by the Taylor polynomial of the first degree at $\boldsymbol{u}_{j_\ell}$

$$T_1[f,\boldsymbol{u}_{j_\ell}](\boldsymbol{u}) = f_{j_\ell} + D_{\boldsymbol{u}-\boldsymbol{u}_{j_\ell}} f(\boldsymbol{u}_{j_\ell}). \tag{13}$$

In fact, the result operator

$$\widetilde{H}_j[f](\boldsymbol{u}) = \sum_{\ell=1}^{3} w_{j,j_\ell}(\boldsymbol{u})\, T_1[f,\boldsymbol{u}_{j_\ell}](\boldsymbol{u}). \tag{14}$$

Proposition 3. Let $f \in C^2(\Omega)$. Then, for each $\boldsymbol{u} \in t_j$, we have

$$\left| f(\boldsymbol{u}) - \widetilde{H}_j[f](\boldsymbol{u}) \right| \leqslant \frac{|D^2 f|_\Omega}{2}\, d_g^2(\boldsymbol{u},\boldsymbol{u}_{j_m}).$$

Proof. From the equation (14), we easily obtain

$$\left| f(\boldsymbol{u}) - \widetilde{H}_j[f](\boldsymbol{u}) \right| \leqslant \sum_{\ell=1}^{3} |w_{j,j_\ell}(\boldsymbol{u})|\, \left| T_1[f,\boldsymbol{u}_{j_\ell}](\boldsymbol{u}) - f(\boldsymbol{u}) \right|, \tag{15}$$

due to the fact that the remainder term between $f(\boldsymbol{u})$ and $T_1[f,\boldsymbol{u}_{j_1}](\boldsymbol{u})$ is bounded as

$$\left| T_1[f,\boldsymbol{u}_{j_\ell}](\boldsymbol{u}) - f(\boldsymbol{u}) \right| \leqslant \frac{|D^2 f|_\Omega}{2}\, d_g(\boldsymbol{u},\boldsymbol{u}_{j_\ell})^2. \tag{16}$$

Finally, by substituting (16) in (15), we obtain the result of Proposition 3. ∎

By combining the surface-triangle-based basis functions (7) with the operators $H_j[f](\boldsymbol{u})$ (10) and with the interpolant $\widetilde{H}_j[f]$ (14), and for any $\mu > 0$ the result surface-Shepard operators are defined as

$$K_\mu[f](\boldsymbol{u}) = \sum_{j=1}^{m} \Phi_{\mu,j}(\boldsymbol{u})\, H_j[f](\boldsymbol{u}), \qquad \widetilde{K}_\mu[f](\boldsymbol{u}) = \sum_{j=1}^{m} \Phi_{\mu,j}(\boldsymbol{u})\, \widetilde{H}_j[f](\boldsymbol{u}). \tag{17}$$

The operators (17) interpolate the function data at each $\boldsymbol{u}_i$, $i = 1,\ldots,n$; this is due to the basis functions property and interpolate properties of local interpolants.

4. Numerical results

In the experiments, in order to check the accuracy of the proposed operators S_μ, K_μ, and $\widetilde{K}_\mu$, we present numerical results for the operators using scattered data on 2-dimensional surfaces. Indeed, this investigation gives a numerical validation of the theoretical results of three operators applied to the surfaces; sphere, cylinder, cone, and a general surface defined by $z = F(x,y)$.

We carried out our various numerical experiments with n Halton scattered data points denoted by X. Data values are taken by the restriction on $\mathcal{M}$ of six test functions, generally used in the literature to test and validate new methods and algorithms, were introduced in [26] and by various authors [4, 6, 27–29]. Six functions are given by:

- Exponential:

$$\begin{aligned} f_1(x,y,z) = {} & 0.75\exp\left(-\frac{(9x-2)^2+(9y-2)^2+(9z-2)^2}{4}\right) \\ & + 0.50\exp\left(-\frac{(9x-7)^2+(9y-3)^2+(9z-7)^2}{4}\right) \\ & + 0.75\exp\left(-\frac{(9x+1)^2}{49}-\frac{(9y+1)^2}{10}-\frac{(9z+1)^2}{10}\right) \\ & - 0.20\exp\left(-(9x-1)^2-(9y-7)^2-(9z-7)^2\right); \end{aligned}$$

- Ccliff:

$$f_2(x,y,z) = \frac{\tanh(9z-9y-9x)+1}{9};$$

- Saddle:
$$f_3(x,y,z) = \frac{(1.25+\cos(5.4y))\cos(6z)}{(6+6(3x-1)^2)};$$
- Steep:
$$f_4(x,y,z) = \frac{\exp((-\frac{81}{4})((x-0.5)^2+(y-0.5)^2+(z-0.5)^2))}{3};$$
- Sphere:
$$f_5(x,y,z) = \frac{\sqrt{64-81((x-0.5)^2+(y-0.5)^2+(z-0.5)^2)}}{9} - 0.5;$$
- Gentle:
$$f_6(x,y,z) = \frac{\exp(-\frac{81}{16}((x-0.5)^2+(y-0.5)^2+(z-0.5)^2))}{3}.$$

Furthermore, we validate the approximation order of the operators K_μ and $\widetilde{K}_\mu$, using five sets of quasi-uniformly distributed points, to generate two types of triangulations, namely Delaunay triangulation and Compact one. Finally, to investigate accuracy of the operators S_μ, K_μ and $\widetilde{K}_\mu$, we compute the maximum absolute error $e_{\max}$, the average error e_{mean}, and the mean square error e_{MS} given by

$$e_{\max} = \max_{1\leqslant i\leqslant n_e} e_i, \qquad e_{\text{mean}} = \frac{1}{n_e}\sum_{i=1}^{n_e} e_i, \qquad e_{\text{MS}} = \sqrt{\frac{\sum_{i=1}^{n_e} {e_i}^2}{n_e}}, \tag{18}$$

where e_i are the pointwise errors computed in absolute value at n_e evaluation points.

For each f of six test functions, we construct $S_\mu[f]$, $K_\mu[f]$, $\widetilde{K}_\mu[f]$ and calculate e_i at the points of a quasi-regular grid and evaluate the errors; maximum, average and mean square (18).

4.1. Numerical results on the sphere

In this subsection, we carried out our numerical experimental in the sphere case, where we consider S^2 the unite sphere, in this case, the geodesic distance d_g and the area of the spherical triangle are defined on S^2 [30] as

$$d_g(\boldsymbol{u},\boldsymbol{v}) = \cos^{-1}(\boldsymbol{u}^t\boldsymbol{v}), \quad \boldsymbol{u},\boldsymbol{v}\in S^2. \tag{19}$$

Now, we carried out an experiment to show the approximation accuracies of the three operators S_2, K_2 and $\widetilde{K}_2$, where we apply those operators to 6 test functions using 1119 Halton points (see Figure 2*a*). Regarding K_2 and $\widetilde{K}_2$, we consider two types of triangulation, Delaunay triangulation and Compact one for each operator (see Figure 2).

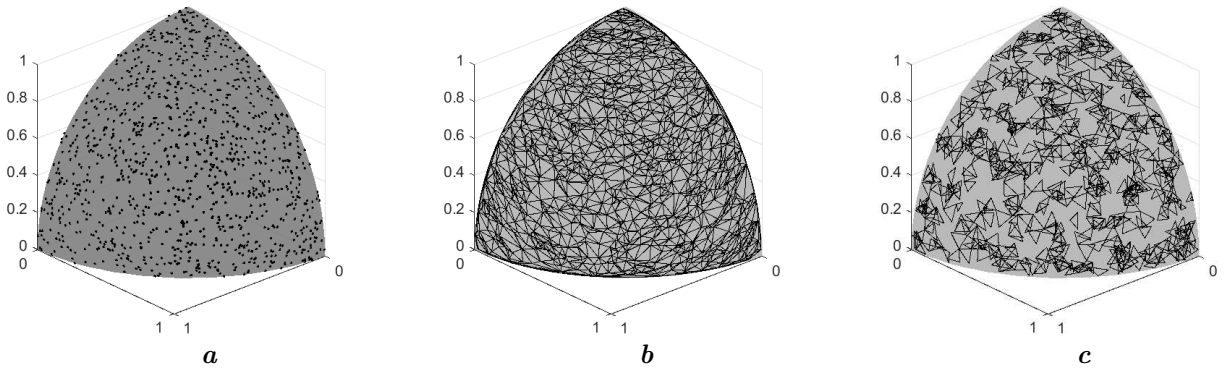

Fig. 2. Set of points on the sphere: 1119 points (***a***), Delaunay triangulation (2226 triangles) (***b***), and Compact triangulation (604 triangles) (***c***).

Table 1 contains the maximum error, mean average error, and square error (18). The errors $\left|S_2[f_i](\boldsymbol{u}) - f_i(\boldsymbol{u})\right|$, $\left|K_2[f_i](\boldsymbol{u}) - f_i(\boldsymbol{u})\right|$ and $\left|\widetilde{K}_2[f_i](\boldsymbol{u}) - f_i(\boldsymbol{u})\right|$ for $i = 1,\ldots,6$; are evaluated at $n_e = 184576$ points.

The obtained numerical results prove that the operators S_2, K_2 and $\widetilde{K}_2$ have a signified accuracy specifically K_2 and $\widetilde{K}_2$ which are better than S_2.

Table 1. Comparison between the operators S_2, K_2 and $\widetilde{K}_2$ applied to the 6 test functions, using the set of 1119 Halton points.

		$S_2[f]$	$K_2[f]$ Delaunay	$K_2[f]$ Compact	$\widetilde{K}_2[f]$ Delaunay	$\widetilde{K}_2[f]$ Compact
f_1	$e_{\max}$	1.2733e-01	9.4037e-03	3.1171e-02	3.7636e-03	1.0927e-02
	e_{mean}	9.7387e-03	3.0412e-04	7.0772e-04	7.1179e-05	1.8550e-04
	e_{MS}	1.7060e-02	7.7245e-04	1.9626e-03	2.1969e-04	6.1227e-04
f_2	$e_{\max}$	9.8447e-02	1.3097e-02	2.8714e-02	7.1515e-03	2.0903e-02
	e_{mean}	1.1497e-02	2.6833e-04	6.2748e-04	1.1022e-04	2.4979e-04
	e_{MS}	1.7675e-02	8.9528e-04	2.0609e-03	3.9405e-04	9.4890e-04
f_3	$e_{\max}$	1.2479e-01	1.2628e-02	2.7175e-02	3.1466e-03	7.5431e-03
	e_{mean}	1.4812e-02	3.5768e-04	8.2982e-04	5.9434e-05	1.4358e-04
	e_{MS}	2.2723e-02	7.7162e-04	1.7613e-03	1.6234e-04	3.6566e-04
f_4	$e_{\max}$	9.0704e-02	3.3433e-03	1.6352e-02	1.9136e-03	4.6729e-03
	e_{mean}	9.3213e-03	1.4731e-04	3.7152e-04	3.8297e-05	1.0667e-04
	e_{MS}	1.4659e-02	3.2256e-04	8.6497e-04	1.0892e-04	2.9629e-04
f_5	$e_{\max}$	2.9804e-01	2.2329e-02	4.1421e-02	7.6448e-03	1.6230e-02
	e_{mean}	1.9561e-02	3.0024e-04	8.0258e-04	5.2200e-05	1.2869e-04
	e_{MS}	2.8668e-02	6.4804e-04	1.5460e-03	1.3410e-04	3.1900e-04
f_6	$e_{\max}$	6.7440e-02	2.3250e-03	8.1282e-03	6.5419e-04	1.7866e-03
	e_{mean}	1.5168e-02	1.6535e-04	3.7932e-04	2.6179e-05	7.6321e-05
	e_{MS}	1.9008e-02	2.8684e-04	6.6235e-04	4.9733e-05	1.4211e-04

4.2. Numerical results on the cylinder

Moving from the considerations on the sphere to those on the cylinder, nothing changes for what concerns the structure of the interpolants and of the cardinal basis functions to be used. In fact, what changes dramatically is the formula of the geodesic distance between two points. Let $\mathcal{C}_y$ be a subset of a right circular cylinder with radius 1 and height 1 defined by

$$\mathcal{C}_y = \big\{(x, y, z) \in [0, 1]^3 : x^2 + y^2 = 1\big\}.$$

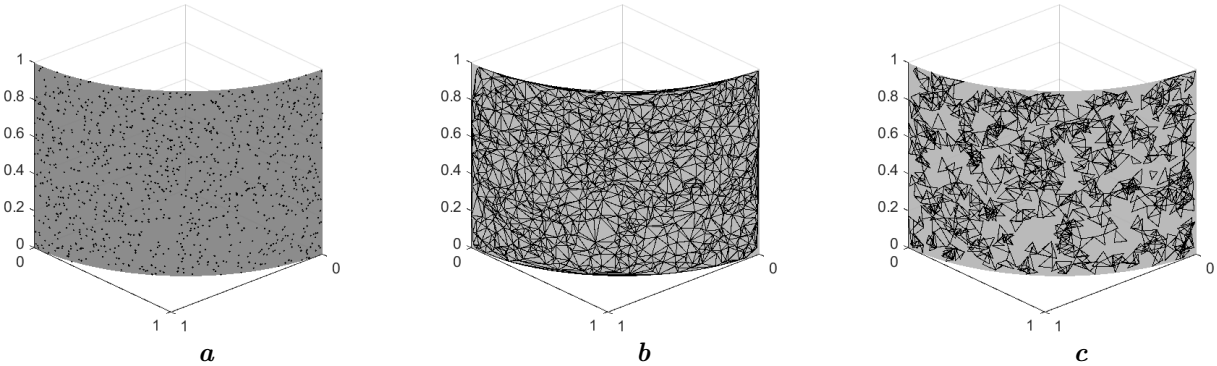

Fig. 3. Set of points on the cylinder: 1101 points (***a***), Delaunay triangulation (2179 triangles) (***b***), and Compact triangulation (614 triangles) (***c***).

The existence of an isometric mapping between $\mathcal{C}_y$ and a rectangle in Euclidean plane geometry allows us to define the geodesic distance and the geodesic triangle area on $\mathcal{C}_y$ based on those of the rectangle in the Euclidean framework.

Let $A = (x_A, y_A, z_A)$, $B = (x_B, y_B, z_B)$ and $C = (x_c, y_c, z_c)$ be three points in $\mathcal{C}_y$.

- The geodesic distance on $\mathcal{C}_y$ between A and B is defined as

$$d_g(A, B) = \sqrt{(z_B - z_A)^2 + \arccos^2(x_A x_B + y_A y_B)}.$$

- The signed area of the geodesic triangle ABC on $\mathcal{C}_y$ is

$$\mathcal{A}_g(A, B, C) = \frac{1}{2}\big(\arcsin(x_A y_B - x_B y_A)(z_C - z_A) - \arcsin(x_A y_C - x_C y_A)(z_B - z_A)\big).$$

In Figure 3, we present the set of points used to generate Delaunay and Compact triangulations on the manifold $\mathcal{C}_y$.

We tested the approximation accuracy of the operators S_4, K_4 and $\widetilde{K}_4$ applied to 6 test functions using Delaunay and Compact triangulations generated by 1101 Halton points on the manifold $\mathcal{C}_y$. Then, we find the same results as in the case of the sphere. Table 2 resumes the obtained results.

Table 2. Comparison between the operators S_4, K_4 and $\widetilde{K}_4$ applied to 6 test functions, using the set of 1101 Halton points.

		$S_4[f]$	$K_4[f]$ Delaunay	$K_4[f]$ Compact	$\widetilde{K}_4[f]$ Delaunay	$\widetilde{K}_4[f]$ Compact
f_1	$e_{\max}$	4.0297e-02	6.3803e-03	1.9926e-02	1.8941e-03	5.3070e-03
	e_{mean}	1.8091e-03	2.3269e-04	5.0549e-04	3.5783e-05	7.7244e-05
	e_{MS}	4.0426e-03	5.5611e-04	1.2880e-03	1.0620e-04	2.4191e-04
f_2	$e_{\max}$	6.1322e-02	2.8341e-02	2.9409e-02	3.3402e-03	6.9304e-03
	e_{mean}	1.5840e-04	5.5099e-05	7.9130e-05	1.0499e-05	1.5667e-05
	e_{MS}	1.3346e-03	5.8432e-04	6.4444e-04	1.0892e-04	1.5187e-04
f_3	$e_{\max}$	6.3083e-02	1.0940e-02	1.8739e-02	1.0286e-03	5.5781e-03
	e_{mean}	3.9710e-03	4.3214e-04	9.7999e-04	3.4033e-05	9.2857e-05
	e_{MS}	6.3955e-03	7.8662e-04	1.7713e-03	6.9288e-05	2.2618e-04
f_4	$e_{\max}$	5.6972e-03	1.1551e-03	2.0926e-03	3.8432e-04	1.5497e-03
	e_{mean}	3.7961e-04	5.1203e-05	1.1049e-04	7.2538e-06	2.0268e-05
	e_{MS}	7.5035e-04	1.0995e-04	2.2690e-04	2.0996e-05	6.6583e-05
f_5	$e_{\max}$	1.3834e-01	4.2462e-02	4.5539e-02	1.6355e-02	1.7347e-02
	e_{mean}	5.2997e-03	3.8642e-04	7.8819e-04	8.8254e-05	1.1585e-04
	e_{MS}	8.7938e-03	1.0776e-03	1.5680e-03	3.7107e-04	3.7603e-04
f_6	$e_{\max}$	1.9031e-02	1.4767e-03	5.2129e-03	7.0725e-04	8.1121e-04
	e_{mean}	2.0968e-03	1.3778e-04	2.8894e-04	2.4456e-05	4.6163e-05
	e_{MS}	2.7998e-03	2.1103e-04	4.6680e-04	4.6232e-05	7.6732e-05

4.3. Numerical results on the cone

Let $\mathcal{C}_o$ be a subset of a right circular cone with radius 1 and height 1 defined by

$$\mathcal{C}_o = \left\{(x,y,z) \in [0,1]^3 \colon\ x^2 + y^2 = z^2\right\}.$$

It is so clear that there is an isometric mapping between $\mathcal{C}_o$ and a flat disk sector with radius $\sqrt{2}$ and central angle $\pi\sqrt{2}/4$ in the geometry of the Euclidean plane. According to this isometry, we define both the geodesic distance and the geodesic triangle area on $\mathcal{C}_o$ with the help of the Euclidean ones on the disk sector.

Let $A = (x_A, y_A, z_A)$, $B = (x_B, y_B, z_B)$ and $C = (x_c, y_c, z_c)$ be three points in $\mathcal{C}_o$.

- The geodesic distance on $\mathcal{C}_y$ between A and B is defined as

$$d_g(A,B) = \sqrt{2}\sqrt{z_A^2 + z_B^2 - 2z_A z_B \cos\left(\frac{\sqrt{2}}{2}\beta(A,B)\right)},$$

where

$$\beta(A,B) = \begin{cases} \arccos\dfrac{x_A x_B + y_A y_B}{\sqrt{x_A^2 + y_A^2}\sqrt{x_B^2 + y_B^2}} & \text{if } \sqrt{x_A^2 + y_A^2}\sqrt{x_B^2 + y_B^2} > 0, \\ 0 & \text{if } \sqrt{x_A^2 + y_A^2}\sqrt{x_B^2 + y_B^2} = 0. \end{cases}$$

- The signed area of the geodesic triangle ABC on $\mathcal{C}_o$ is

$$\mathcal{A}_g(A,B,C) = z_B z_C \sin\left(\frac{\sqrt{2}}{2}\gamma(B,C)\right) + z_A z_B \sin\left(\frac{\sqrt{2}}{2}\gamma(A,B)\right) + z_A z_C \sin\left(\frac{\sqrt{2}}{2}\gamma(C,A)\right),$$

where

$$\gamma(A,B)=\begin{cases}\arcsin\dfrac{x_Ay_B-x_By_A}{\sqrt{x_A^2+y_A^2}\sqrt{x_B^2+y_B^2}} & \text{if } \sqrt{x_A^2+y_A^2}\sqrt{x_B^2+y_B^2}>0,\\ 0 & \text{if } \sqrt{x_A^2+y_A^2}\sqrt{x_B^2+y_B^2}=0.\end{cases}$$

Here, we perform our numerical experiments with 1105 points on the surface $\mathcal{C}_o$ (see Figure 4), and we test the operators S_2, K_2 and $\widetilde{K}_2$ applied to 6 test functions using Delaunay and Compact triangulations. Table 3 shows the approximation accuracy results.

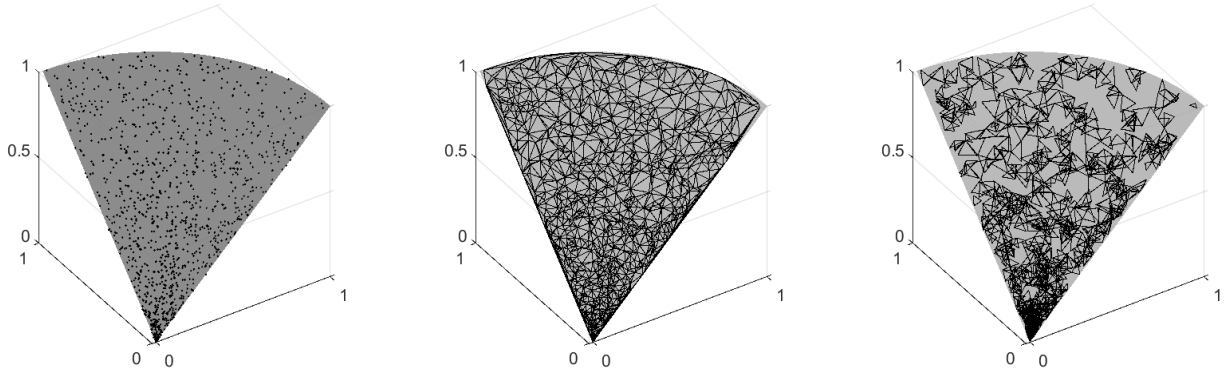

a ***b*** ***c***

Fig. 4. Set of points on the cone: 1105 points (***a***), Delaunay triangulation (2192 triangles) (***b***), and Compact triangulation (614 triangles) (***c***).

Table 3. Comparison between the operators S_2, K_2 and $\widetilde{K}_2$ applied to the 6 test functions, using the set of 1105 Halton points.

		$S_2[f]$	$K_2[f]$ Delaunay	$K_2[f]$ Compact	$\widetilde{K}_2[f]$ Delaunay	$\widetilde{K}_2[f]$ Compact
f_1	$e_{\max}$	1.6727e-01	1.5286e-02	3.2557e-02	1.6854e-02	5.9845e-02
	e_{mean}	4.0405e-02	8.5168e-04	2.1688e-03	2.9055e-04	7.0954e-04
	e_{MS}	4.8415e-02	1.5900e-03	3.8147e-03	1.0004e-03	2.7193e-03
f_2	$e_{\max}$	7.1859e-02	1.1448e-02	1.2223e-02	5.5784e-03	4.1594e-03
	e_{mean}	7.1650e-03	2.3672e-04	5.2821e-04	5.6826e-05	1.0364e-04
	e_{MS}	1.0582e-02	6.1519e-04	1.1647e-03	1.7913e-04	2.8276e-04
f_3	$e_{\max}$	1.6243e-01	5.6826e-03	9.4809e-03	2.0364e-03	3.0962e-03
	e_{mean}	1.7309e-02	2.7380e-04	6.8687e-04	6.6305e-05	1.4186e-04
	e_{MS}	2.6831e-02	4.9643e-04	1.1919e-03	1.4964e-04	2.9348e-04
f_4	$e_{\max}$	8.8312e-02	5.9272e-03	1.4304e-02	1.3539e-03	3.3301e-03
	e_{mean}	1.0221e-02	1.9145e-04	5.0902e-04	3.7534e-05	9.9155e-05
	e_{MS}	1.5504e-02	4.1992e-04	1.1572e-03	9.6550e-05	2.5133e-04
f_5	$e_{\max}$	3.8225e-01	4.6490e-02	4.3121e-02	1.8835e-02	1.7079e-02
	e_{mean}	2.1273e-02	3.5805e-04	1.0191e-03	5.3950e-05	7.1797e-05
	e_{MS}	3.4399e-02	8.8836e-04	2.2863e-03	2.7585e-04	2.9722e-04
f_6	$e_{\max}$	7.2985e-02	3.9272e-03	9.9883e-03	6.7673e-04	1.5594e-03
	e_{mean}	1.6673e-02	1.8548e-04	4.5685e-04	2.5592e-05	5.9266e-05
	e_{MS}	2.1728e-02	3.3460e-04	8.5508e-04	5.0115e-05	1.2183e-04

4.4. Numerical results on surfaces defined by $z = F(x, y)$

Consider a surface $\mathcal{M}$ given by

$$\mathcal{M}=\{(x,y,F(x,y));\ (x,y)\in[0,1]^2\}.$$

We assume that $F\in C^1([0,1]^2)$. To test the performance of our interpolation method, we need to compute the geodesic distance on general surfaces. Unfortunately, finding a geodesic distance is another critical point.

A curve $\gamma\colon [0,1] \to [0,1]^2$ gives a curve $F \circ \gamma : [0,1] \to \mathcal{M}$ on the surface $\mathcal{M}$, its length is given by

$$L[F \circ \gamma] = \int_0^1 \left\| (F \circ \gamma)'(t) \right\|_{\mathbb{R}^3} dt.$$

A geodesic on $\mathcal{M}$ is a curve $F \circ \gamma$, with $\gamma = (\gamma_1, \gamma_2)$, which γ satisfy the system of the second order differential equations, called geodesic equations

$$\ddot{\gamma}_k + \sum_{i,j} \Gamma_{ij}^k \dot{\gamma}_i \dot{\gamma}_j = 0, \tag{20}$$

where Γ_{ij}^k are the Christoffel symbols of the second kind (for more detail see [31,32]). The system (20) can be solved theoretically and uniquely, but there are serious difficulties. To solve equations of geodesics (20) on a parametric surface, we can use Matlab or Python. To test our interpolants on surfaces, we focus on $\mathcal{M}$ with $F(x,y) = \cos(2\pi x)\sin(\pi y)$. As interpolation nodes, we take some sets of n uniformly random Halton data points, originally contained in the unit square $[0,1]^2$ Figure 5. The test functions to be interpolated are taken from the restriction to $\mathcal{M}$ of the trivariate functions already considered for the sphere, cylinder, and cone. But we report only the numerical results obtained considering f_1 and f_2. The interpolation errors computed for the interpolants $S_2[f]$, $K_2[f]$, and $\widetilde{K}_2[f]$ are shown in Table 4.

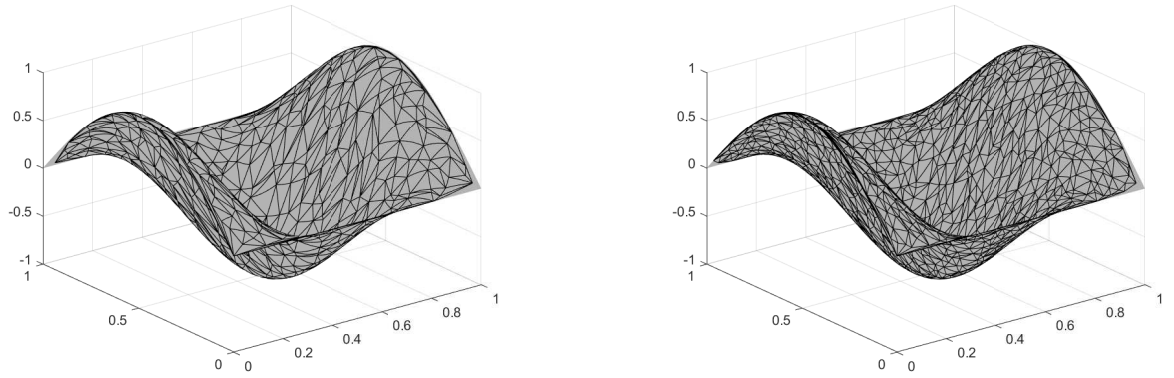

Fig. 5. Set of points on the surface: 500 points (Delaunay triangulation (982 triangles)) (***a***), 1000 points (Delaunay triangulation (1980 triangles)) (***b***).

Table 4. Comparison between the operators S_2, K_2 and $\widetilde{K}_2$ applied to the f_1 and f_2 test functions, using the set of $n = 500, 1000$ Halton points.

	n		$S_2[f]$	$K_2[f]$ Delaunay	$\widetilde{K}_2[f]$ Delaunay
f_1	500	$e_{\max}$	9.1213e-02	4.2527e-02	2.285e-02
		e_{mean}	7.9868e-03	2.8788e-03	7.2655e-04
		e_{MS}	1.4143e-02	5.3807e-03	1.8804e-03
f_1	1000	$e_{\max}$	2.0622e-02	2.1234e-02	1.6841e-02
		e_{mean}	6.4215e-04	6.2321e-04	2.9026e-04
		e_{MS}	3.0741e-04	2.1767e-04	1.0132e-04
f_2	500	$e_{\max}$	2.6874e-02	5.4760e-03	4.3641e-03
		e_{mean}	2.0382e-03	8.2657e-04	2.1632e-04
		e_{MS}	3.1623e-03	2.1018e-04	4.5934e-04
f_2	1000	$e_{\max}$	1.1292e-02	7.4530e-03	2.4576e-03
		e_{mean}	3.7123e-04	3.6801e-04	6.1532e-05
		e_{MS}	1.0113e-03	6.1453e-04	7.875e-05

5. Conclusion and future works

The results of three numerical tests presented in Section 4 validate the theoretical results developed in Sections 2 and 3. Indeed, we obtained the desired approximation order of the operators K_μ and $\widetilde{K}_\mu$ using either Delaunay triangulation or Compact triangulation. In this work, the numerical results present a good approximation accuracy in the local scale using $e_{\max}$ and globally according to e_{mean} and e_{MS} as well. Summarising, this paper presents a powerful interpolation method to get accurate functional approximation with less computational cost. This work will be also very helpful in many application fields such as the numerical resolution of partial differential equations with new methods.

In future work, we will generalize and develop this study by working in a more general framework and by presenting new triangulation strategies adapted to this type of interpolation problem. Furthermore, these new interpolation strategies will be a strong point of the Shepard method, which would be an effective tool in many real applications, especially in space engineering, telecommunications, meteorology, astronomy, air quality, and air traffic.

[1] Meijering E. A chronology of interpolation: from ancient astronomy to modern signal and image processing. Proceedings of the IEEE. **90** (3), 319–342 (2002).

[2] Shepard D. A two-dimensional interpolation function for irregularly-spaced data. Proceedings of the 1968 23rd ACM national conference. 517–524 (1968).

[3] Liszka T. An interpolation method for an irregular net of nodes. International Journal for Numerical Methods in Engineering. **20** (9), 1599–1612 (1984).

[4] McLain D. H. Drawing contours from arbitrary data points. The Computer Journal. **17** (4), 318–324 (1974),

[5] Farwig R. Rate of convergence of Shepard's global interpolation formula. Mathematics of Computation. **46** (174), 577–590 (1986).

[6] Renka R. J., Brown R. Algorithm 792: Accuracy Tests of ACM Algorithms for Interpolation of Scattered Data in the Plane. ACM Transactions on Mathematical Software (TOMS). **25** (1), 78–94 (1999).

[7] Thacker W. I., Zhang J., Watson L. T., Birch J. B., Iyer M. A., Berry M. W. Algorithm 905: SHEPPACK: Modified Shepard algorithm for interpolation of scattered multivariate data. ACM Transactions on Mathematical Software (TOMS). **37** (3), 1–20 (2010).

[8] Karandashev K., Vaníček J. A combined on-the-fly/interpolation procedure for evaluating energy values needed in molecular simulations. The Journal of chemical physics. **151** (17), 174116 (2019).

[9] Farrahi G. H., Faghidian S. A., Smith D. J. An inverse approach to determination of residual stresses induced by shot peening in round bars. International Journal of Mechanical Sciences. **51** (9–10), 726–731 (2009).

[10] Alfeld P., Neamtu M., Schumaker L. L. Fitting scattered data on sphere-like surfaces using spherical splines. Journal of Computational and Applied Mathematics. **73** (1–2), 5–43 (1996).

[11] Baramidze V., Lai M. I., Shum C. K. Spherical splines for data interpolation and fitting. SIAM Journal on Scientific Computing. **28** (1), 241–259 (2006).

[12] Cavoretto R., De Rossi A. A spherical interpolation algorithm using zonal basis functions. Proceedings of the International Conference on Computational and Mathematical Methods in Science and Engineering (CMMSE09). **1**, 258–269 (2009).

[13] Fasshauer G. E. Adaptive least squares fitting with radial basis functions on the sphere. Mathematical Methods for Curves and Surfaces. 141–150 (1995).

[14] Fasshauer G. E., Schumaker L. L. Scattered data fitting on the sphere. Mathematical Methods for Curves and Surfaces II. 117–166 (1998).

[15] Meyling R. H. J. G., Pfluger P. R. B-spline approximation of a closed surface. IMA Journal of Numerical Analysis. **7** (1), 73–96 (1987).

[16] Pottmann H., Eck M. Modified multiquadric methods for scattered data interpolation over a sphere. Computer Aided Geometric Design. **7** (1–4), 313–321 (1990).

[17] Sloan I. H., Womersley R. S. Constructive polynomial approximation on the sphere. Journal of Approximation Theory. **103** (1), 91–118 (2000).

[18] Womersley R. S., Sloan I. H. How good can polynomial interpolation on the sphere be? Advances in Computational Mathematics. **14** (3), 195–226 (2001).

[19] Allasia G., Cavoretto R., De Rossi A. Hermite–Birkhoff interpolation on scattered data on the sphere and other manifolds. Applied Mathematics and Computation. **318**, 35–50 (2018).

[20] Dyn N., Narcowich F. J., Ward J. D. A Framework for Interpolation and Approximation on Riemannian. Approximation Theory and Optimization: Tributes to MJD Powell. 133–144 (1997).

[21] Dyn N., Narcowich F. J., Ward J. D. Variational principles and Sobolev-type estimates for generalized interpolation on a Riemannian manifold. Constructive Approximation. **15** (2), 175–208 (1999).

[22] Narcowich F. J. Generalized Hermite interpolation and positive definite kernels on a Riemannian manifold. Journal of Mathematical Analysis and Applications. **190** (1), 165–193 (1995).

[23] Horemuž M., Andersson J. V. Polynomial interpolation of GPS satellite coordinates. GPS Solutions. **10** (1), 67–72 (2006).

[24] Alexander R., Alexander S. Geodesics in Riemannian manifolds-with-boundary. Indiana University Mathematics Journal. **30** (4), 481–488 (1981).

[25] Corral M. Vector calculus. Independent (2013).

[26] Renka R. J. Multivariate interpolation of large sets of scattered data. ACM Transactions on Mathematical Software. **14** (2), 139–148 (1988).

[27] Franke R. Scattered data interpolation: Tests of some methods. Mathematics of Computation. **38** (157), 81–200 (1982).

[28] Hubbert S., Morton T. M. Lp-error estimates for radial basis function interpolation on the sphere. Journal of Approximation Theory. **129** (1), 58–77 (2004).

[29] Nouisser O., Zerroudi B. Modified Shepard's method by six-points local interpolant. Journal of Applied Mathematics and Computing. **65** (1), 651–667 (2021).

[30] Todhunter I. Spherical trigonometry, for the use of colleges and schools: with numerous examples. Macmillan (1863).

[31] Boykov Y., Kolmogorov V. Computing geodesics and minimal surfaces via graph cuts. Proceedings Ninth IEEE International Conference on Computer Vision. **3**, 26–33 (2003).

[32] Baek J., Deopurkar A., Redfield K. Finding Geodesics on Surfaces. Dept. Comput. Sci., Stanford Univ., Stanford, CA, USA, Tech. Rep. (2007).

Інтерполяція розсіяних даних на двовимірній поверхні за допомогою методу Шепарда

Зерроді Б.[1], Тайек Х.[2,3], Ель Харрак А.[3]

[1] *Лабораторія інженерних наук, Факультет природничих наук, Університет Ібн Зор, Агадір, Марокко*
[2] *SMAD, FPL, Університет Абдельмалека Ессааді, Тетуан, Марокко*
[3] *MMA, FPL, Університет Абдельмалека Ессааді, Тетуан, Марокко*

У цій статті розглядається задача інтерполяції розсіяних даних на двовимірних поверхнях шляхом пропозиції поширення методу Шепарда та його модифікованої версії на поверхні. Кожен запропонований оператор є лінійною комбінацією базисних функцій, коефіцієнти яких є значеннями функції або її розкладів Тейлора першого порядку в точках інтерполяції з використанням як функціональних, так і похідних даних. Для демонстрації ефективності інтерполяції наведено чисельні тести, де декілька чисельних результатів показують хорошу точність наближення запропонованого оператора.

Ключові слова: *інтерполяція розсіяних даних; алгоритми інтерполяції; методи Шепарда; апроксимація многовидів; поверхневий трикутник.*